# Photogrammetry- and LiDAR-based Multi-temporal Point Cloud Models and Digital Elevation Models for Landslide Investigation in Hong Kong - Feasibility and Challenges

Y T A Chan[1*], L Liu[1], W Hou[2], R Tsui[3]

[1]The Chinese University of Hong Kong, Hong Kong, China
[2]GeoRisk Solutions Limited, Hong Kong, China
[3]Aurecon Hong Kong Limited, Hong Kong, China

*Corresponding author
doi: https://doi.org/10.21467/proceedings.133.13

**ABSTRACT**

In adapting to rapid urban development and changing climate, the geotechnical industry is shifting towards harnessing digital technologies in Natural Terrain Hazard Study (NTHS) for landslide investigation. In this paper, we adopted a new digital method using multi-temporal point cloud models and digital elevation models derived from various available resources for the assessment of landslide source volume and dimensions. These resources include (1) historical aerial photographs from territory-wide aerial photographic survey carried out by the Lands Department, (2) project-specific UAV photographic and video surveys, and (3) the territory-wide airborne LiDAR surveys data. Two case studies from the Fei Ngo Shan area, Hong Kong, were carried out. Case 1 involves two recent landslides that occurred in 2005, and Case 2 involves a cluster of eight recent landslides that occurred in 2020. All these ten landslides were carefully investigated using conventional methods (e.g., field measurement or API) by GEO and GeoRisk Solutions, respectively. These investigation results were taken as legacy records for a comparison with the results derived from our adopted digital method. The comparison shows that the landslide source volume derived from the digital method is similar to the legacy record. This paper assessed the feasibility and accuracies of aligning and comparing digital models derived from multi-sources for landslide studies.

**Keywords:** Landslide, Photogrammetry, LiDAR

## 1 Introduction

### 1.1 Background

Landslides are a common and devastating type of natural disasters which often cause loss of life and irreparable damage. In Hong Kong, 60% of its terrain is hilly or mountainous with steep slopes. As a result, NTHS is a compulsory risk management strategy for the safe and cost-effective utilization and development of lands.

Conventional approaches to investigate the landslide source volume typically utilize direct field-based measurements, i.e., hand-held tape measures, to estimate and record the extent and the dimensions of a landslide scar. In spite of the long history of this application, several major limitations still exist. First, the unavailability of instant measurement after the landslide, given the time required to gain a safe field access to the scar, slows down the response in risk mitigation. Second, the conventional assumption of ellipsoidal landslide geometry may not fit the actual natural terrain landslides in Hong Kong (Hou et al., 2021).

With the rapid advancement in technology, the potential to take new approaches and utilize innovative developments in landslide studies arises. Airborne photogrammetry and LiDAR in particular, can overcome some of the limitations of the conventional methodology. By building and



Proceedings DOI: 10.21467/proceedings.133; Series: AIJR Proceedings; ISSN: 2582-3922; ISBN: 978-81-957605-1-0

analyzing a multi-temporal digital model, a fast, cost-effective, relatively accurate and safe remote survey for landslide features can be provided.

The key objective of this paper is to construct pre- and post-failure high-resolution and accurately georeferenced point cloud models (PCM) and digital elevation models (DEM) for the 2005 and 2020 landslides in Fei Ngo Shan area. By aligning and comparing these 3D models (i.e., pre- and post-failure), the landslide failure volume together with its source dimensions can be computed, section profiles can be generated and 3D presentations can be provided. This paper aims to show the potential of digital measures and to encourage the NTHS practitioners in Hong Kong to adopt relevant digital measures.

## 1.2 Study Area

This paper studies ten landslide features in total, i.e., two features from the 2005 Fei Ngo Shan landslides and eight features from the 2020 Fei Ngo Shan landslides (Figure 1).

The 2005 Fei Ngo Shan landslide occurred on the natural hillside near Fei Ngo Shan service reservoir at about 6 a.m. on 21 August 2005 (Maunsell, 2008), which was possibly triggered by heavy and prolonged rainfall. The landslide event comprised a major channelized debris flow landslide (i.e., Landslide No. 1) involving a failure volume of about 3,350 m³, and a smaller landslide (i.e., Landslide No. 2), involving a failure volume of about 180 m³ (Maunsell, 2008). A Landslide No. 3 was reported by Maunsell (2008). However, this Landslide No. 3 is not covered by this paper due to its comparatively distant location. The 2020 Fei Ngo Shan landslide comprised a cluster of eight landslides (i.e., RC15 to RC22), which were most likely triggered by a heavy rainstorm between 2:00 am and 6:00 am on 6 June 2020 (GRS, 2021). These landslides were debris avalanches with estimated source volumes ranging from 13 m³ to 144 m³ (GRS, 2021).

## 1.3 Regional Geology

The study area was predominantly underlain by fine ash vitric tuff from the Mount Davis Formation that forms part of the Lower Cretaceous Repulse Bay Volcanic Group. The Mount Davis Formation is at least 500 m thick and comprises variably lapilli-bearing, coarse ash crystal tuff, with some eutaxite and sandstone beds at the type locality. Bands of eutaxitic crystal-bearing fine ash vitric tuff and thin bands of quartzphyric rhyolite dykes are aligned sub-parallel to the strike of the volcanic strata (Figure 1).

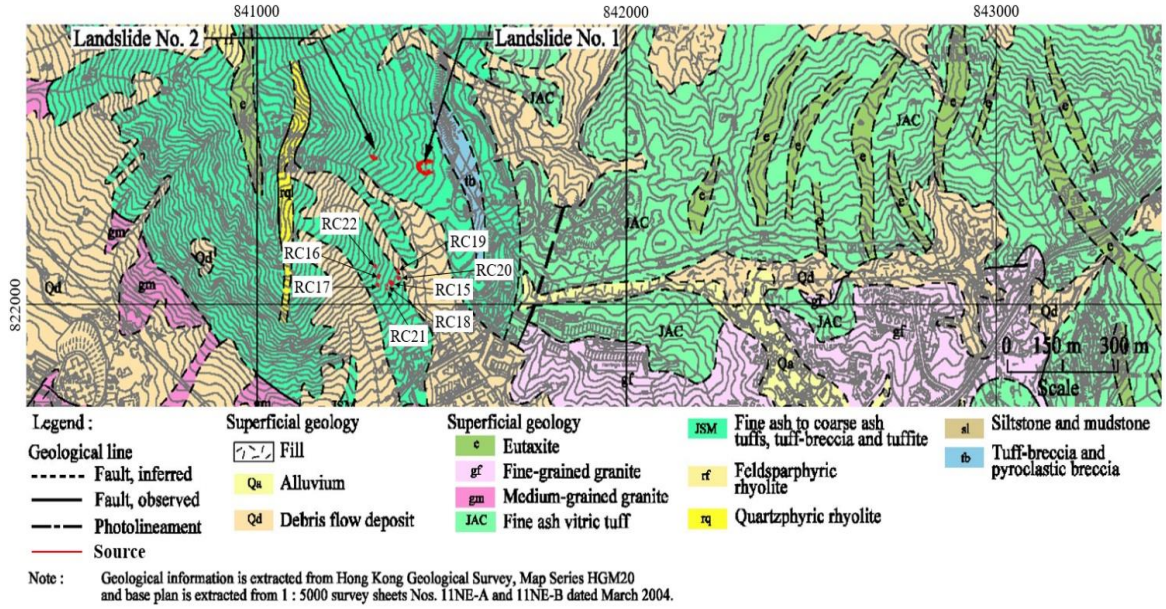


**Figure 1:** Location of landslide source areas indicated on the regional geological map

Proceedings DOI: 10.21467/proceedings.133
ISBN: 978-81-957605-1-0

Series: AIJR Proceedings
ISSN: 2582-3922

## 2 Methodology & Data Collection

### 2.1 Data Collection

For case study 1 (i.e., the 2005 features), pre- and post-failure point cloud models were constructed using historical aerial photographs. For case study 2 (i.e., the 2020 features), the pre-failure point cloud model was obtained directly from the 2020 territory wide airborne LiDAR survey. The post-failure point cloud model was constructed from project-specific UAV survey (including photos and videos). More details are provided in Table 1 and Table 2.

**Table 1:** Digital sources applied for each 3D model

| | **Pre-failure model** | **Post-failure model** |
|---|---|---|
| **The 2005 landslide** | Historical aerial photos taken in Mar, Apr, May 2005 & Sep 2004 (Lands Department, 2021) | Historical aerial photos taken in Oct 2005 (Lands Department, 2021) |
| **The 2020 landslide** | The 2020 LiDAR survey (GEO, n.d.) | UAV survey in Sep 2021 (Hou et al., 2021) |

**Table 2:** Historical aerial photos applied for the 2005-point clouds modelling (Lands Department, 2021)

| | **Pre-failure model** | | | | **Post-failure model** | |
|---|---|---|---|---|---|---|
| **Date** | 07/05/05 | 03/04/05 | 08/03/05 | 11/09/04 | 25/10/05 | |
| **Flying Height (ft.)** | 3500 | 2500 | 4000 | 4000 | 4000 | |
| **Selected Aerial Photograph No.** | CW64629<br>CW64630<br>CW64631<br>CW64632 | CW64003<br>CW64004<br>CW64005 | CW63614<br>CW63615<br>CW63616<br>CW63617<br>CW63618<br>CW63619 | CW58943<br>CW58944<br>CW58945<br>CW58946<br>CW58947<br>CW58948 | CW66184<br>CW66185<br>CW66186<br>CW66187<br>CW66210<br>CW66211<br>CW66212<br>CW66213 | CW66214<br>CW66215<br>CW66216<br>CW66217<br>CW66224<br>CW66225<br>CW66226<br>CW66227 |

#### 2.1.1 Historical Aerial Photographs

In order to construct point cloud models on Agisoft Metashape Professional Edition (Agisoft Metahsape Pro), we adopted four sets of aerial photographs from several flying heights on four different dates before the occurrence of the landslide on 21st August 2005. For the post-failure point cloud, the aerial photos were taken on 25th October of the same year, more than two months after the debris flow, from 4,000 feet flying height.

Obviously, the lower the flying height, the closer to our study feature, meaning a higher resolution: 4,000 feet flying height produces a high enough resolution for our purpose. Originally, we intended to use aerial photographs taken at the same height and date on a single flying path, but there were not enough of these photographs to provide a full coverage of the study area. Therefore, we decided to select aerial photos taken from different flying heights of several flying paths on different dates. Although they have different flying heights from more than one time periods, this does not violate the principle of SfM photogrammetry and has been shown to have limited impact on the quality of the constructed point cloud for our purpose.

The study used the freely available digital version colour frames (DAP-L0) aerial photographs at 300 dpi resolution downloaded from Lands Department (2021).

#### 2.1.2 UAV

We adopt the UAV survey of the 2020 Fei Ngo Shan landslide conducted by GRS (2021), with a DJI Mavic Air 2 equipped with a camera. A series of photos and several videos were taken during the survey. UAV photos and a series of consecutive frames extracted from video clips were used to build the model with software Agisoft Metahsape Pro. The photos acquired from the UAV are accompanied by GPS coordinates stored as metadata embedded in the photo files.

#### 2.1.3 Airborne LiDAR (ALS)

LiDAR mounted on an airborne platform produces higher frequency EM pulses, typically Near-infrared (wavelength 1064 nm) or Green (wavelength 532 nm), then records the reflectance from the ground surface. The light's travel time is then measured by an optical telescope mounted on the same platform. After that, the travel time is converted to distance, from which a LiDAR point cloud can be constructed.

The 2020 territory-wide Airborne LiDAR survey in Hong Kong is an open-source data provided by Geotechnical Engineering Office (GEO), Civil Engineering and Development Department. The data was collected from Dec 2019 to Feb 2020. LAS format of the LiDAR Data was used and data covering the map sheets nos. 11NE8A, 11NE8B, 11NE8C and 11NE8D were required to cover the regional area of the study landslide features.

### 2.2 Methodology

#### 2.2.1 Structure from Motion (SfM) Data Processing

Structure from Motion (SfM), with multiview stereo, is a crucial technique derived from photogrammetry, surveying and computer vision, using overlapping images to establish hyper-scale three-dimensional landform models for observing multi-temporal geomorphic processes (Eltner & Sofia, 2020).

Traditionally, landslide inventory maps are prepared by stereoscopic aerial photograph interpretations (API) and field validation. Fiorucci et al (2018) claimed that API by stereoscope can be interrupted by shadows, obstructing the photographic elements typical of landslides. This hinders the recognition and mapping of the landslides (Fiorucci et al., 2018). Furthermore, the detailed observations made from an interpretation of aerial photographs are qualitative and subjective, making it impossible to perform precise analytic data analysis.

By contrast, photogrammetry technique, along with LiDAR geodetic observations method, offers detailed topographic information for hazards analyses and possible instantaneous monitoring through observing large morphological changes (Chan, 2021). Depending on the desired level of accuracy, aerial photography can be converted into a PCM or a DEM for further calculations and analysis within a short period of time in general cases.

#### 2.2.2 Georeferencing

Georeferencing of the 3D point cloud models was carried out in software CloudCompare (CC). Two georeferencing tools, i.e., Align and Transformation, were applied in the study.

For the 2005 landslide models, both the pre-failure and the post-failure models were aligned to the LiDAR point cloud (i.e., the reference cloud). For point-pair registration, a minimum of three ground control points (GCP) can exactly map each raster point to the target location with a first-order transformation (Esri, n.d.). In this study, four control points with one at each corner were used for covering the area of the study features. These control points were selected from corners of man-made features.

Proceedings DOI: 10.21467/proceedings.133
ISBN: 978-81-957605-1-0

Series: AIJR Proceedings
ISSN: 2582-3922

The 2020 UAV model was initially generated with Agisoft Metahsape Pro, and possessed correct x, y coordinates and inaccurate z coordinates due to the limitation of the drone equipment. Therefore, adjustment of z-value was completed in CC. A z-axis translation of 298.5 upward was applied to align the 2020 UAV model to the LiDAR model (i.e., the reference model). The accuracy of the translation was validated by professional judgment of the good matching of the landslide crowns and the pre-failure ground.

#### 2.2.3 Digital Elevation Model (DEM)

DEM is defined as the ground, or bare earth, and contains only topography, whereas a Digital Surface Model (DSM) is a first return surface and includes tree canopy and buildings (Esri, n.d.). In our study, DEM is constructed for volume calculation since only the non-vegetated landslide scars are of concern, compared against the bare surface model, for source volume calculation.

After all the preparation works of point cloud processing, point cloud cleaning, and georeferencing of the pre- and post-failure landslide 3D models of 2005 and 2020, a DEM with 0.01 m resolution can finally be derived through rasterization on ArcGIS.

Due to the 2020 LiDAR survey adopting the Hong Kong 1980 Grid Coordinate System, we must convert the Coordinate Reference System (CRS) to Hong Kong 1980 Grid before making other calculations or measurements. This step is crucial because LiDAR is either used for comparison directly or as a reference model indirectly.

#### 2.2.4 Volume and Dimension Estimation

To estimate the landslide source volume, two platforms, i.e., CloudComapre (CC) and ArcGIS Pro (ArcGIS), were used. The main purpose of comparing the CC-computed with the ArcGIS-computed source volumes is to confirm that the point cloud-based volume calculations obtained in CC are as reliable as calculating volume using DEM (raster) data in ArcGIS. To estimate the landslide source length, width and depth, "Point Picking" tool on CC were used. Once determined to be accurate by comparing to legacy, the whole process including both volume and dimension estimation can be simplified into only working on CC after deriving PCMs on Agisoft Metahsape Pro.

In CC, the pre-failure and the post-failure model of each year was compared to deduce the 2.5D Volume of the landslides. 2.5 spatial dimensions defines as a uniformly spaced grid that records the elevation on a cell-by-cell basis (Verhoeven et al., 2021). According to the same study, truly 3D digital surfaces are less used in geo-sciences because of the limitations of most GIS software till this very day with their display and analysis. The first step of pre-processing is to segment the source volume of each landslide. Then, it is necessary to segment or filter the vegetation and the noise from the landslide scar given that these signals sum the contribution of each cell and affect the calculation. After that, the "2.5D Volume" tool rasterized the point clouds, generated the 2.5D raster with one height value added to each grid cell, projected the clouds inside, and deduced the volume between two 2.5D clouds (CloudCompareWiki, 2015).

In ArcGIS Pro, the segmented source areas of the landslides in LAS format were firstly converted into rasters. After the conversion, the spatial analyst tool, Raster Calculator, was used to execute a Map Algebra expression: (Pre-failure model – Post-failure model) * Pixel Area. Finally, data within this volume raster was exported into a table for further analysis.

#### 2.2.5 Accuracy Assessment

Ultimately, the failure volume, the profiles of the landslides and the calculated source area dimensions are compared to the legacy records in "*Geo Report No. 233*" for the 2005 landslides and "*Using UAV-based Technology to Enhance Landslide Investigation*" for the 2020 landslides, as a follow-up georeferencing uncertainty analysis adopting two different methods.

For the alignment accuracy of the 2005 landslide PCMs to the LiDAR reference PCM, root mean square error (RMSE) is used to describe how consistent the transformation is between the different control points (Esri, n.d.). RMSE is one of the standard ways to measure the error of a model, lower values indicating better accuracy and thus a better model performance.

Another method for assessing the accuracy of the 2005 and the 2020 landslide PCM is by the Gaussian (Normal) distribution of the signed distances directly between the stable region, i.e., excluding the landslides scars, of the pre- and post-failure point clouds. The mean value in Gaussian distribution fitting indicates the statistics on how close the cloud distances are to one another and 0 denotes a perfect fit with no gap. Thus, the convergence towards 0 signals an ideal model. The standard deviation (SD) simply conveys the dispersion of the points in clouds.

## 3 Results

### 3.1 Volume Estimation and Area Dimension

**Table 3:** A comparison of source volumes (in $m^3$), widths (in m), lengths (in m) and depths (in m) of the 2005 and 2020 landslides, using point cloud data processed by CC and DEM data processed by ArcGIS.

| Year | Landslide | Legacy Volume | Estimated Volume by CC | ΔVolume (Legacy-CC) | Estimated Volume by ArcGIS | ΔVolume (CC-ArcGIS) | Legacy Width | Estimated Width | ΔWidth (Legacy-CC) | Legacy Length | Estimated Length | ΔLength (Legacy-CC) | Legacy Depth | Estimated Depth | ΔDepth (Legacy-CC) |
|---|---|---|---|---|---|---|---|---|---|---|---|---|---|---|---|
| 2005 | NO1 | 3350.0 | 2679.5 | 670.5 | 2677.9 | 1.6 | 32.0 | 48.8 | -16.8 | 54.0 | 64.2 | -10.2 | 5.0 | 5.0 | 0.0 |
| 2005 | NO2 | 180.0 | 160.4 | 19.6 | 159.6 | 0.8 | 10.0 | 12.1 | -2.1 | 18.0 | 23.3 | -5.3 | 2.0 | 1.9 | 0.1 |
| 2020 | RC15 | 144.0 | 139.0 | 5.0 | 130.8 | 8.2 | 11.0 | 11.4 | -0.4 | 10.0 | 8.3 | 1.7 | 2.5 | 2.1 | 0.4 |
| 2020 | RC16 | 81.6 | 81.0 | 0.6 | 78.2 | 2.8 | 12.0 | 10.0 | 2.0 | 13.0 | 7.9 | 5.1 | 1.5 | 2.6 | -1.1 |
| 2020 | RC17 | 70.0 | 36.5 | 33.5 | 39.3 | -2.8 | 8.5 | 7.2 | 1.3 | 10.5 | 9.3 | 1.2 | 1.5 | 1.4 | 0.1 |
| 2020 | RC18 | 13.1 | 1.3 | 11.8 | -2.1 | 3.4 | 5.0 | 2.1 | 2.9 | 5.0 | 2.2 | 2.8 | 1.0 | -1.0 | 2.0 |
| 2020 | RC19 | 41.2 | 43.2 | -2.0 | 49.2 | -6.0 | 7.5 | 7.2 | 0.3 | 7.0 | 4.5 | 2.5 | 1.5 | 1.9 | -0.4 |
| 2020 | RC20 | 57.8 | 55.5 | 2.3 | 62.6 | -7.1 | 13.0 | 10.1 | 2.9 | 8.5 | 5.7 | 2.8 | 1.0 | 2.0 | -1.0 |
| 2020 | RC21 | 15.7 | 16.7 | -1.0 | 14.1 | 2.6 | 5.0 | 4.2 | 0.8 | 6.0 | 5.1 | 0.9 | 1.0 | 1.3 | -0.3 |
| 2020 | RC22 | 61.8 | 58.4 | 3.4 | 54.7 | 3.7 | 7.5 | 7.2 | 0.3 | 10.5 | 10.3 | 0.2 | 1.5 | 1.7 | -0.2 |

The source volumes are derived by ArcGIS and CC respectively while the widths, lengths and depths are all measured in CC. The changes in volume and dimensions are computed by the results generated on CC subtracted from legacy records. An additional comparison between the CC-derived and the ArcGIS-derived volume is shown in Table 3.

Regardless of the computing software, subtracting the post-failure model from the pre-failure model gives us a reduction in volume. Take RC18, for example: its negative estimated volume by ArcGIS indicates a source volume increase, which reveals an anomaly in the result because landslides should normally be associated with a volume drop. The cause of this will be further explained in the upcoming Discussion section. For any negative delta volume, width, length or depth, it means that particular result acquired via CC is larger than legacy.

It is observed that the difference in the estimated source volume between the two methods ranges from 0.8 to 8.2 $m^3$. For 2005 landslide No.1, our digital approach of the estimated source volume by CC is 670.5 $m^3$ less than the physical measurement record in the *GEO Report No. 233* whereas landslide No.2 is only 19.6 $m^3$ less than legacy. However, the large variation in landslide No.1 is due to the concrete cover on its landslide scar with unknown thickness summing to a certain volume. For the 2020 Fei Ngo Shan landslides, the mean of the volume difference is 6.7 $m^3$ and the median is 2.8 $m^3$. Among

Proceedings DOI: 10.21467/proceedings.133
ISBN: 978-81-957605-1-0

Series: AIJR Proceedings
ISSN: 2582-3922

all the 2020 landslides, RC16 has the smallest difference of 0.6 m³ while RC17 has the largest difference of 33.5 m³. The source volumes are summarized in Figure 2.

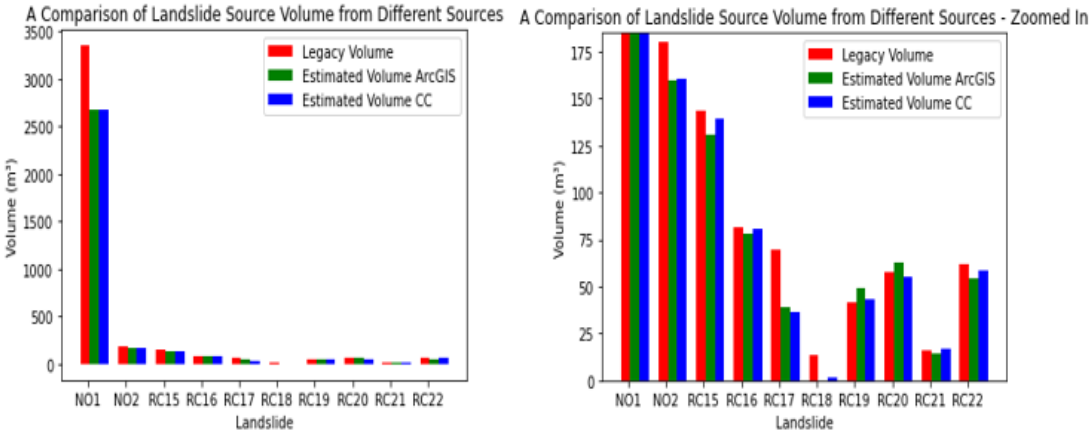


**Figure 2:** Bar charts of the estimated source volumes. The left is the overview while the right is zoomed in to 180 m³

Out of the 10 landslides, only the legacy volumes in landslides No.1, No.2, RC17 and RC18 are intuitively larger than our estimations.

The overall performance in source area measurement is reasonable and not far from the past records if excluding the significant longer length and width of the 2005 No.1 landslide. In general, the mean of the difference in width is -0.9 m, in length is 0.2 m, in depth is 0.04 m.

### 3.2 Landslide Profiles

Applying terrain profile for analytical analysis is a common application for observing the failure from the side view. Instead of the traditional line profile, Cross Section in CC was used to extract polygonal contours in each slice to give a more realistic look to the profiles of the point clouds.

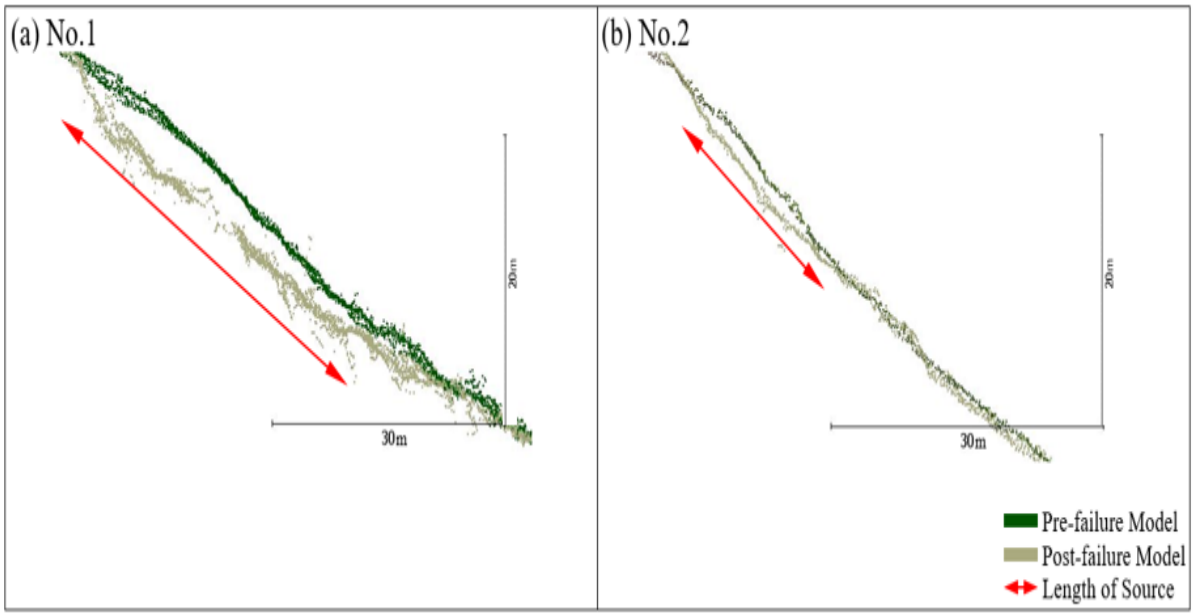


**Figure 3:** Source area profiles of the 2005 landslides, showing the pre-failure model compared against the post-failure model, derived from historical aerial photographs.

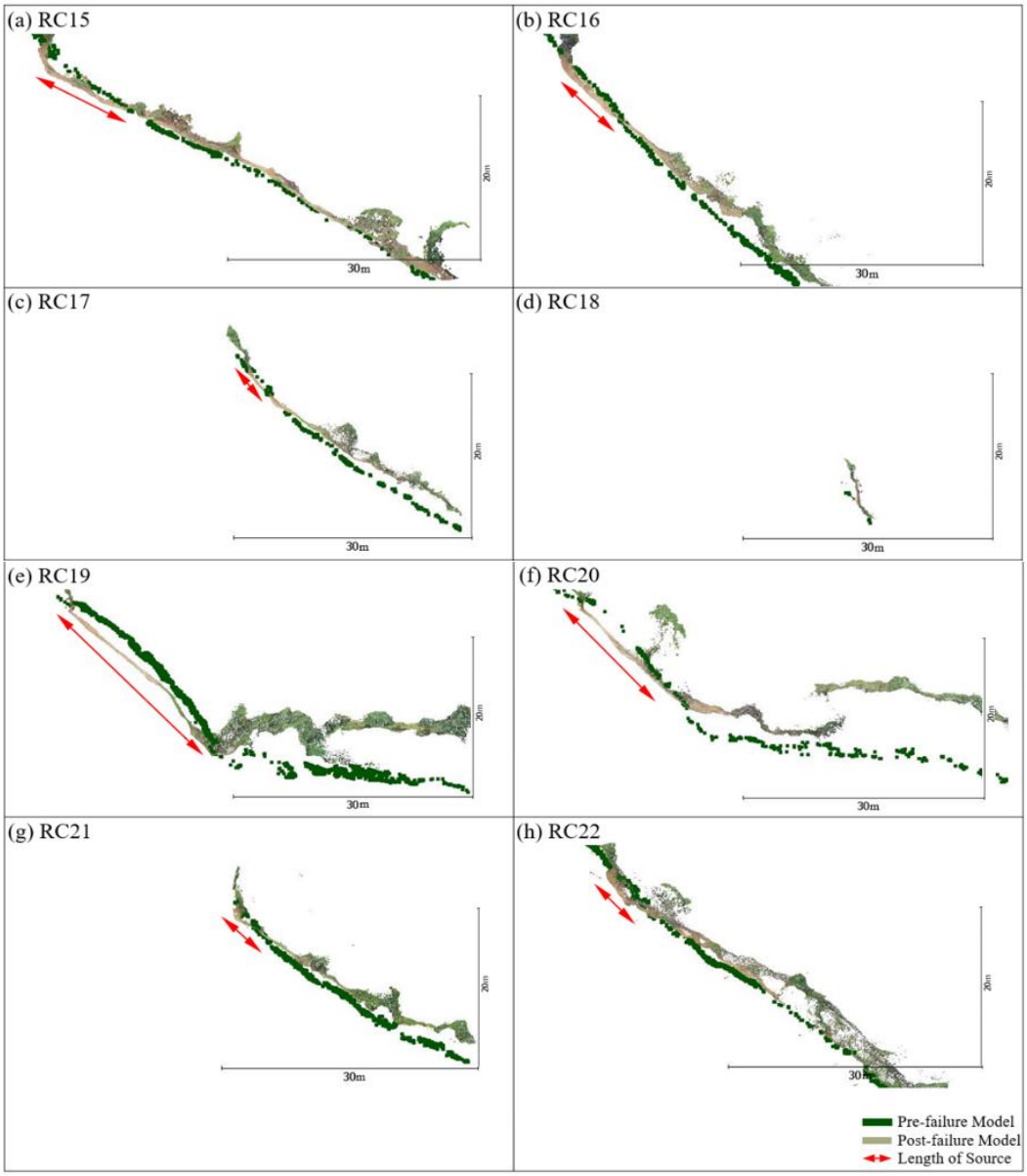


**Figure 4:** Source area profiles of the 2020 landslides, showing the LiDAR pre-failure model compared with the UAV-SfM-derived post-failure model. For (f) RC18, since the pre-failure model is lying beneath the post-failure model, no source area can be found

### 3.3 Georeferencing Uncertainty

The georeferencing accuracy of the 2005 pre- and post-failure PCMs aligned to the LiDAR reference PCM assessed by RMSE, as well as the 2005 and the 2020 landslide PCMs assessed by Gaussian distribution, are summarized into Table 4 and 5 respectively.

**Table 4:** The final RMSE of the 2005 pre-failure and the post-failure models aligned to LiDAR respectively

| | **Pre-failure Model aligned to LiDAR (m)** | **Post-failure Model aligned to LiDAR (m)** |
|---|---|---|
| **The 2005 landslide** | 0.91 | 2.30 |

**Table 5:** The Gaussian mean and standard deviation of the signed distances of the 2005 and the 2020 pre- and post-failure PCMs

| | **Mean (m)** | **Standard Deviation (m)** |
|---|---|---|
| **The 2005 landslide** | -2.85 | 1.22 |
| **The 2020 landslide** | -0.65 | 1.04 |

Proceedings DOI: 10.21467/proceedings.133
ISBN: 978-81-957605-1-0

Series: AIJR Proceedings
ISSN: 2582-3922

# 4 Discussions

## 4.1 Use of Data

The sensory data used in this study, Airborne LiDAR and aerial photographs acquired from various remote sensing platforms such as UAV, contain potential estimation errors originating from their data generation methods and flight operations (Hsieh et al., 2016). According to the same study, the elevation error of airborne LiDAR survey is about 0.15-0.3 m and for aerial photogrammetry is about 0.2-1.3 m. The inaccuracy in the elevation of the UAV-derived point clouds is encountered in the study but the difference is 298.5 m lower than the actual. The explanation for this is that UAV relies on the Inertial Measuring Units and the Global Navigation Satellite System (GNSS) for positioning and orientation. If GNSS signals suffer from interference, it also affects the entire pose estimation of the UAV and causes altitude errors (Forte et al., 2021). To conclude, the constraint in this study is the variation of positional accuracy of various techniques, i.e., aerial photos, LiDAR used, which affects the result of parameter estimation.

## 4.2 Georeferencing Uncertainty

Recalling the RMS accuracy of the pre-failure model aligned to LiDAR is 0.91 m and the final RMSE of the post-failure model aligned to LiDAR is 2.30 m. The positive RMSE indicates the predicted value overestimates the actual value, which partly can be contributed by the variations between the vegetated SfM PCM and the bare ground LiDAR model. The larger RMSE of the post-failure model, comparing to the pre-failure model, can be attributable to the elevation difference of the landslide scars between the post-failure PCM and the reference LiDAR model.

Despite such RMSE values providing valuable insight into overall georeferencing performance, they do not expose the spatial variability for detailed PCM or DEM analyses as uncertainty estimates for topographic change detection can lose validity in regions of steep topography (James et al., 2017). Therefore, the RMSE values above do not necessarily mean the positioning accuracy is unsatisfactory for the purpose of studying geomorphological changes caused by landslides and its insight is currently restricted by our limited understanding of SfM survey uncertainties (James et al., 2017). Although the positioning accuracy directly depends on the accuracy of GCPs, it is challenging to achieve perfect georeferencing. Furthermore, a low RMSE should not be confused with an accurate registration, because the transformation may still contain significant errors due to a poorly entered control point. The significant transformation errors can be improved by selecting more GCPs with equal quality (Esri, n.d.).

Reciting the georeferencing accuracy for 2005 landslides models, the Gaussian mean is -2.85 m with a SD of 1.22 m, meaning that the post-failure PCM is 2.85 m lower than the post-failure PCM with a dispersion of 1.22 m relative to its mean. For the 2020 UAV-derived point cloud versus the vegetated LiDAR point cloud, the mean is -0.65 m with a SD of 1.04 m, meaning that the LiDAR model is 0.65 m lower than the SfM PCM with a dispersion of 1.04 m relative to its mean. To sum up, the general georeferencing performance of the 2020 3D models is better than the 2005's. It is because the horizontal georeferencing uncertainty of the UAV-derived PCM has been reduced given that the horizontal GPS positioning of the UAV source is accurate, neglecting the data generation and the operation errors. By contrast, the uncertainties of the pre- and the post-failure 3D models of 2005 based solely on aerial photos at natural hillsides are uncertain, as it depends on the time to take the photos and the quality of the photos, or other potential human errors involved. Thus, the analysis of 2005 landslides may involve a higher degree of uncertainty in landslide volume determination.

When it comes to the georeferencing methodology, Airborne LiDAR has a key role in this study by acting as a reference cloud, as well as acting as a post-failure model in 2020 for generating source volume. However, the above methodologies were based on the assumption of LiDAR being both

horizontally and vertically accurate. In reality, the LiDAR collection process consists of positional (X-Y-Z) error, where the horizontal (X-Y) error is typically much greater than the vertical error (Hodgson & Bresnahan, 2004). The height accuracy of airborne LiDAR measurement technology may be as high as 13 cm while horizontal accuracy may be as high as 20 cm (Ren et al., 2016). Moreover, it is worth noting that the LiDAR point cloud may be sparse at some depth and thus provide insufficient point cloud data, preventing precise computing of the landslide volume.

### 4.3 Volume and Dimension Estimation

The estimated volumes computed by ArcGIS Pro and CC are not the same, but as close as a difference of 0.8 - 8.2 $m^3$. Both platforms undergo point cloud rasterization before calculation, adopting the same segments of source area input, with the same rationale of the formula: product of the difference in elevation and the grid or pixel area. Despite all those similarities, the variations between the two software algorithms may have triggered the distinct values in landslide source volumes. The range of difference has been proven to be reasonable, in such case, it fulfils the main objective of comparing the CC-computed source volume with the ArcGIS-computed source volume is to verify that the results obtained in CC are indeed as reliable. Therefore, we would recommend taking the CC methodology, which has the simplest procedure, as a common practice in digital approaches to measuring landslide source volumes.

For record comparison, there is a relatively large difference in the 2005 No.1 and No.2 landslides, together with the 2020 RC17 and RC18 landslides, among all the legacy volumes and our estimated volumes. Only the landslides with a difference of larger than 10 $m^3$ have been evaluated for possible improvements. Landslide No.1 can be explained by the concrete cover on its landslide scar with unknown thickness which could have counted towards the 670.5 $m^3$ difference, even though its width and length are 16.8 and 10.2 m larger than the records stated in GEO Report No. 233. The volume gap of landslide No.2 still could not be narrowed down further from 19.6 $m^3$ since it already adopts a wider and longer dimension. Similarly, RC17 in 2020 already has a wider and longer dimension than the legacy but the volume estimation is still 30.7 $m^3$ smaller than the result obtained by GRS (2021). Based on other volumes being mostly consistent, the actual RC17 source volume may be controversial. On the other hand, RC18 can be rejected as a null result, not only because the LiDAR density is exceptionally sparse in that particular shadow position resulting in poor airborne LiDAR survey coverage, but also because the post-failure model has a higher elevation than the pre-failure model. In other words, this creates an anomalous source volume increase, as estimated by ArcGIS Pro, or an atypically low volume as measured by CC.

### 4.4 Possible Improvements

There are two possible improvements can be made in future applications.

First, purchase of GeoTIFF, defined as a tagged image file format with geographic information, from the Lands Department would be an option for constructing a point cloud model or a DEM. This could save time from 3D point cloud georeferencing, together with providing a higher resolution of the digital aerial photos than the freely available 300 dpi version.

Second, to achieve a more accurate source volume estimation, filtering the vegetation signals from the landslide scars is another optional procedure; the detailed steps can be referenced in Hou et al. (2021).

Within this context, the photogrammetry and LiDAR-based methodologies used to construct 3D models in this study are far from maturity, and still have great potential for development.

Proceedings DOI: 10.21467/proceedings.133
ISBN: 978-81-957605-1-0

Series: AIJR Proceedings
ISSN: 2582-3922

## 5 Conclusion & Future Application

Among all the landslides, 2020 RC16 has the smallest difference of 0.6 $m^3$ while 2005 No.1 has the largest difference of 670.5 $m^3$. 60% of the investigated landslides have variations of less than 10 $m^3$ from the legacy records. For the georeferencing accuracy, the Gaussian mean and the SD of the signed distances directly between the 2005 pre- and the post-failure point cloud models are -2.85 m and 1.22 m while 2020 has an even better mean of -0.65 m with a SD of 1.04 m. The outcomes of the study are therefore robust.

All in all, NTHS requires professional knowledge and expertise, and thus the source area dimension segmentation is subject to individual professional judgements. Nevertheless, this study serves as a comprehensive guide and a comparison to past results. The consistent records from the traditional field-based measurements in *GEO Report No. 233* have validated the feasibility of this remote sensing approach. On the other hand, by applying the same digital method of using a UAV-based SfM photogrammetry to construct a landslide 3D model, the acceptable range of result variations between this study and Hou et al. (2021) has proven the consistency of this methodology. Therefore, not only has this adventurous digital approach demonstrated its practicability, but also it reveals a trend of shifting from rasters towards point clouds, more dependence in the future on processing voxels directly instead of pixels.

On top of industrial application, generating accurate landslide volumes will be important for risk management and future research, in adapting to new challenges brought by growth and development in Hong Kong, and global climate change. It is worth mentioning that the importance of the landslide clusters in Fei Ngo Shan is that they were triggered by a 1-in-2000-year rainfall event (GRS, 2021; Hou et al., 2021). Under the conventional practice, the total volume of the 2020 cluster can be treated as a 1-in-2000-year landslide event. Therefore, all the data acquired and processed, along with and the relevant analysis, revealed can be used as a benchmark for a future Quantitative Risk Assessment (QRA) practice.

These remote sensing digital modelling techniques aided by GIS can possibly complement the NTHS and enhance future investigations, bringing lower costs but higher efficiency, accuracy and effectiveness.

## 6 Declarations

### 6.1 Acknowledgements

We would like to express our special thanks to Mr. Ken Grimes from the English Language Teaching Unit, The Chinese University of Hong Kong (CUHK), for his language advice throughout the project, and Dr. WONG Kwan Kit from Department of Geography and Resource Management, CUHK, for his advice on georeferencing methodology. We acknowledge the provision of LiDAR survey data and other relevant information from the Geotechnical Engineering Office of the Civil Engineering and Development Department of the HKSAR Government. This paper is extracted from the undergraduate Final Year Project (FYP) of one of the authors, Y. T. Agnes CHAN. This FYP is a collaboration project between the Earth System Science Programme (ESSC), CUHK and the Hong Kong based geotechnical engineering consultant, GeoRisk Solutions Limited (GRS). The project is supervised by Prof. Lin LIU of ESSC, CUHK and co-supervised by Dr. Wenzhu HOU of GRS.

### 6.2 Publisher's Note

## References


Chan, A. (2021). Volcano Geodesy [Unpublished manuscript]. The Chinese University of Hong Kong.

CloudCompareWiki. (2015, October 19). 2.5D Volume. 2.5D Volume - CloudCompareWiki. Retrieved March 27, 2022, from https://www.cloudcompare.org/doc/wiki/index.php?title=2.5D_Volume

Eltner, A., and G. Sofia (2020), Chapter 1 - Structure from motion photogrammetric technique, Developments in Earth Surface Processes, 23, 1–24, doi:10.1016/b978-0-444-64177-9.00001-1.

Esri (n.d.), Creating raster DEMs and DSMs from large lidar point collections, Lidar solutions in ArcGIS. Available from: https://desktop.arcgis.com/en/arcmap/10.3/manage-data/las-dataset/lidar-solutions-creating-raster-dems-and-dsms-from-large-lidar-point-collections.htm#ESRI_SECTION1_7ABD98654A49411FB44CF0920B23F427 (Accessed 7 December 2021)

Esri. (n.d.). Overview of georeferencing. Overview of georeferencing-ArcGIS Pro | Documentation. Retrieved March 28, 2022, from https://pro.arcgis.com/en/pro-app/latest/help/data/imagery/overview-of-georeferencing.htm

Fiorucci, F., F. Ardizzone, A. C. Mondini, A. Viero, and F. Guzzetti (2018), Visual interpretation of stereoscopic NDVI satellite images to map rainfall-induced landslides, Landslides, 16(1), 165–174, doi:10.1007/s10346-018-1069-y.

Forte, M., Neto, P., Thé, G., & Nogueira, F. (2021). Altitude Correction of an UAV assisted by Point Cloud Registration of LIDAR SCANS. Proceedings of the 18th International Conference on Informatics in Control, Automation and Robotics, 485–492. https://doi.org/10.5220/0010583004850492

GeoRisk Solutions Limited (GRS) 2021. Study Of Natural Terrain Hazards For A Major Drainage Catchment (MDC), At Fei Ngo Shan, Kowloon [internal report for GEO]

Geotechnical Engineering Office (GEO) (n.d.). GEO Data For Public Use. Open data - geo, CEDD, HKSARG. Retrieved March 30, 2022, from https://www.geomap.cedd.gov.hk/GEOOpenData/eng/Default.aspx

Geotechnical Engineering Office (GEO) 2021. Landslide Risk Management and the Role of Quantitative Risk Assessment Techniques. Geotechnical Engineering Office, Civil Engineering and Development Department, Hong Kong Government.

Hodgson, M. E., & Bresnahan, P. (2004). Accuracy of airborne lidar-derived elevation. Photogrammetric Engineering & Remote Sensing, 70(3), 331–339. https://doi.org/10.14358/pers.70.3.331

Hou, W., J. R. Hart, R. Tsui, A. Ng, and C. Cheung (2021), Using UAV-based technology to enhance landslide investigation, Available from: https://www.researchgate.net/publication/352177443_Using_UAV-based_Technology_to_Enhance_Landslide_Investigation (Accessed 3 December 2021)

Hsieh, Y.-C., Chan, Y.-C., & Hu, J.-C. (2016). Digital Elevation Model differencing and error estimation from multiple sources: A case study from the Meiyuan Shan landslide in Taiwan. Remote Sensing, 8(3), 199. https://doi.org/10.3390/rs8030199

James, M. R., Robson, S., & Smith, M. W. (2017). 3-D uncertainty-based topographic change detection with structure-from-motion photogrammetry: Precision maps for ground control and directly georeferenced surveys. Earth Surface Processes and Landforms, 42(12), 1769–1788. https://doi.org/10.1002/esp.4125

Maunsell Geotechnical Services Limited (Maunsell) (2008). Detailed Study of the 21 August 2005 Debris Flow on the Natural Hillside near Fei Ngo Shan Service Reservoir. GEO Report No. 233.Geotechnical

Lands Department (2021), Hong Kong Map Service 2.0, Available from: https://www.hkmapservice.gov.hk/OneStopSystem/home (Accessed 5 December 2021)

Ren, H. C., Yan, Q., Liu, Z. J., Zuo, Z. Q., Xu, Q. Q., Li, F. F., & Song, C. (2016). Study on analysis from sources of error for Airborne Lidar. IOP Conference Series: Earth and Environmental Science, 46, 012030. https://doi.org/10.1088/1755-1315/46/1/012030

Verhoeven, G. J., Santner, M., & Trinks, I. (2021). From 2d (to 3D) to 2.5D – not all gridded digital surfaces are created equally. ISPRS Annals of the Photogrammetry, Remote Sensing and Spatial Information Sciences, VIII-M-1-2021, 171–178. https://doi.org/10.5194/isprs-annals-viii-m-1-2021-171-2021